Research Square

Preprints are preliminary reports that have not undergone peer review.
They should not be considered conclusive, used to inform clinical practice,
or referenced by the media as validated information.

Synthesis and Structural Characterization of Amine-Functionalized Zinc- and Copper-Based Metal–Organic Frameworks (Zn-BDC-NH2 and Cu-BDC-NH2)

Charles Dike

charlesdike075@gmail.com

Federal University Otuoke

Abosede Olufunsho

Federal University Otuoke

TUNDE SAMUEL ADEWALE

Federal University Otuoke

Research Article

Keywords: metal–organic framework, amine functionalization, 2-aminoterephthalic acid, solvothermal synthesis, FTIR, X-ray diffraction

Posted Date: November 10th, 2026

DOI: https://doi.org/10.21203/rs.3.rs-11318521/v1

License: This work is licensed under a Creative Commons Attribution 4.0 International License.
Read Full License

Additional Declarations: No competing interests reported.

Abstract

Metal–organic frameworks (MOFs) functionalized with pendant amine groups are of growing interest as tunable, low-cost adsorbent platforms because their pore surfaces can be engineered to interact selectively with polar and ionizable pollutants. In this study, amine-functionalized zinc-based (Zn-BDC-NH2 MOF) and copper-based (Cu-BDC-NH2 MOF) metal–organic frameworks were synthesized from 2-aminoterephthalic acid (BDC-NH2) and the corresponding metal nitrate precursors using a simple, conventional solution-based route in ethanol buffered with sodium acetate at near-neutral pH. The two products were characterized by Fourier transform infrared (FTIR) spectroscopy, powder X-ray diffraction (XRD), and scanning electron microscopy (SEM). FTIR spectra of both materials showed disappearance of the free carboxylic acid C=O stretch of the parent linker and its replacement by an asymmetric/symmetric carboxylate (COO−) doublet, together with new low-frequency bands assigned to Zn–O and Cu–O stretching, confirming metal–carboxylate coordination, while retained C–N bands confirmed that the –NH2 functionality survived framework assembly in both cases. XRD patterns confirmed the crystallinity of both products, with Cu-BDC-NH2 MOF displaying a greater number of well-resolved reflections extending to higher diffraction angles and a smaller Debye–Scherrer crystallite size (≈51 nm) than Zn-BDC-NH2 MOF (≈80 nm). SEM revealed markedly different morphologies: coarse, angular, plate-like aggregates for Zn-BDC-NH2 MOF versus fine, globular, densely packed nanoparticle clusters for Cu-BDC-NH2 MOF. Together, these results establish a reproducible, low-cost synthetic route to two structurally distinct amine-functionalized MOFs bearing free –NH2 groups, providing a structurally characterized platform for subsequent pollutant-adsorption applications.

1. Introduction

Metal–organic frameworks (MOFs) are crystalline coordination materials built from metal ions or metal-containing clusters connected by organic ligands into extended one-, two-, or three-dimensional networks (Batten et al., 2013; Furukawa et al., 2013). Their modular construction allows both the metal node and the organic linker to be varied independently, so that pore size, framework topology, and pore-wall chemistry can, in principle, be tailored for a chosen application. This tunability, together with the high surface areas and permanent porosity that many MOFs display, has driven substantial interest in their use for gas storage and separation, catalysis, sensing, and environmental remediation (Furukawa et al., 2013; Li et al., 2012).

A key strategy for directing MOF performance toward a specific application is functionalization of the pore-lining surface with reactive chemical groups. Functional groups such as amino, hydroxyl, carboxylate, sulfonate, and thiol moieties can be incorporated either directly, by using a pre-functionalized organic linker during synthesis, or afterward, through post-synthetic modification of an already-formed framework (Cohen, 2012; Deng et al., 2010). According to Pearson's hard–soft acid–base (HSAB) framework, nitrogen-donor groups behave as borderline-to-hard bases with a strong affinity for many transition-metal and heavy-metal species, while oxygen-donor and sulfur-donor groups show complementary hard- and soft-base character, respectively (Li et al., 2019; Wu et al., 2019; Zhang et al.,

2017; Zhao et al., 2019). Amine-functionalized MOFs in particular have been widely explored because the free –NH2 group, once retained on the pore wall after framework assembly, can participate in hydrogen bonding, coordination, and electrostatic interactions with polar or ionizable guest molecules, in addition to any interactions offered by the metal centres themselves.

2-Aminoterephthalic acid (BDC-NH2), the amine-substituted analogue of terephthalic acid, is a convenient linker for introducing this functionality because it retains the two carboxylate donor groups needed for metal coordination while carrying a pendant amine group that is not directly involved in framework bonding and therefore remains available within the pore. Zinc and copper were selected as the metal centres for this study because Zn(II) and Cu(II) are inexpensive, readily available, and form carboxylate-bridged frameworks with terephthalate-type linkers under mild solution conditions (Li et al., 1998), while offering contrasting coordination geometries and Lewis-acid character that would be expected to influence both the crystallinity and the surface chemistry of the resulting materials.

Conventional solvothermal and hydrothermal routes remain the most widely used methods for MOF synthesis, typically involving reaction of a metal salt with an organic linker in a suitable solvent under controlled temperature, time, and pH (Stock & Biswas, 2012). Compared with high-temperature autoclave methods, a low-temperature, buffered solution-based route offers a simpler and more accessible synthetic entry point, particularly where specialized solvothermal equipment is not readily available, while still permitting reticular self-assembly of metal ions and carboxylate linkers into ordered, porous coordination networks (Rubio-Martinez et al., 2017; Yaghi et al., 2003).

Although the successful synthesis of amine-functionalized MOFs is frequently reported, rigorous structural confirmation, particularly evidence that the amine group survives framework assembly intact and that the product is genuinely a new coordination compound rather than a physical mixture of unreacted starting materials, is essential before such materials can be reliably deployed as adsorbents. The present work therefore reports the synthesis of amine-functionalized zinc-based (Zn-BDC-NH2 MOF) and copper-based (Cu-BDC-NH2 MOF) metal–organic frameworks from a common linker, 2-aminoterephthalic acid, using a simple buffered solution-based route, and their structural characterization by FTIR spectroscopy, powder XRD, and SEM. The specific objectives were (i) to synthesize both amine-functionalized MOFs by a reproducible, low-cost solution-based method, and (ii) to confirm framework formation, retention of the –NH2 functional group, phase purity/crystallinity, and surface morphology of the two products, providing a structurally validated platform for the pollutant-adsorption studies reported separately.

2. Materials and Methods

2.1 Chemicals and Reagents

Zinc(II) nitrate hexahydrate [Zn(NO3)2·6H2O], copper(II) nitrate trihydrate [Cu(NO3)2·3H2O], 2-aminoterephthalic acid (BDC-NH2), N,N-dimethylformamide (DMF), and absolute ethanol were obtained

from Macklin (Shanghai Macklin Biochemical Technology Co., Ltd., China) and used as received without further purification. Deionized water, sodium hydroxide, and glacial acetic acid (for buffer preparation) were sourced from the Federal University Otuoke (FUO) laboratory. All glassware was cleaned and oven-dried prior to use.

2.2 Preparation of Sodium Acetate Buffer

Sodium hydroxide pellets (4.00 g) were dissolved in approximately 50 mL of deionized water with continuous magnetic stirring. Glacial acetic acid was measured separately and added slowly to the sodium hydroxide solution with continuous stirring until a homogeneous solution formed. The pH of the resulting acetate buffer was checked with a calibrated digital pH meter and adjusted dropwise with dilute NaOH or acetic acid to the target value of pH 7, then stored at room temperature in a labelled reagent bottle until use.

2.3 Synthesis of Zn-BDC-NH2 MOF

A conventional, solution-based synthesis was used to prepare the zinc-based amine-functionalized MOF. 2-Aminoterephthalic acid (0.18 g) was dissolved in 10 mL of ethanol with stirring, after which 0.5 mL of the pH 7 sodium acetate buffer was added dropwise with continuous stirring until a homogeneous brown solution formed. Separately, zinc(II) nitrate hexahydrate (0.29 g) was dissolved in 5 mL of ethanol. The zinc solution was added gradually to the linker/buffer solution under continuous stirring, and the resulting mixture was stirred for approximately 5 h, yielding a homogeneous yellowish-brown solution. The mixture was sonicated to improve dispersion and contact between the reacting species, filtered to remove undissolved particles, and the filtrate was transferred to a clean, labelled container and left to age/crystallize at room temperature for 5–7 days, during which coordination between Zn2 + and the carboxylate/amine functional groups of the linker proceeded to give nucleation and crystal growth of Zn-BDC-NH2 MOF. The solid product was recovered and dried in preparation for characterization.

2.4 Synthesis of Cu-BDC-NH2 MOF

Cu-BDC-NH2 MOF was prepared following an identical procedure to that described in Section 2.3, substituting copper(II) nitrate trihydrate (0.24 g in 5 mL ethanol) for the zinc precursor. Addition of the copper solution to the linker/buffer solution produced a homogeneous brownish-grey mixture after 5 h of stirring. Sonication, filtration, and 5–7-day room-temperature aging/crystallization were carried out as described above to obtain the Cu-BDC-NH2 MOF product.

2.5 Characterization

Powder X-ray diffraction (XRD) patterns were recorded over a 2θ range of 2–70° using CuKα radiation to determine the crystallinity and phase characteristics of the two products. Fourier transform infrared (FTIR) spectra of the free linker, the two MOFs, were recorded over 4000–350 cm − 1 to identify functional groups and confirm metal–linker coordination. Scanning electron microscopy (SEM) was used, following gold sputter-coating of the samples, to examine surface morphology, particle shape, and aggregation behaviour at accelerating voltages of 15–20 kV. UV–Visible spectroscopy (200–800 nm)

was additionally used to probe the electronic transitions associated with metal–ligand interaction in the synthesized frameworks. Synthesis was carried out at the Directorate of Research and Quality Assurance, Federal University Otuoke; XRD, SEM, UV–Visible, and FTIR analyses were conducted at the University of Ibadan Chemistry Laboratory.

3. Results and Discussion

3.1 Physical Recovery of the Synthesized MOFs

Reaction of Zn(NO3)2·6H2O and Cu(NO3)2·3H2O, respectively, with the BDC-NH2 linker in sodium-acetate-buffered ethanol, followed by aging/crystallization, yielded fine crystalline powders of Zn-BDC-NH2 MOF and Cu-BDC-NH2 MOF after filtration. As shown below, the FTIR, XRD, and SEM data obtained for both products are mutually consistent with the formation of new, ordered metal–carboxylate coordination frameworks rather than a simple physical mixture of the unreacted metal salt and free organic linker.

3.2 FTIR Spectroscopic Analysis

The FTIR spectrum of the free BDC-NH2 linker displayed a broad absorption centred at 3433 cm − 1, attributed to overlapping N–H stretching of the aromatic amine and O–H stretching of the carboxylic acid groups; a band at 1633 cm − 1 assigned to the protonated carboxylic acid C = O stretch together with aromatic C = C ring stretching; a strong, sharp band at 1027 cm − 1 assigned to C–N stretching and aromatic C–H bending; and bands at 771, 548, and 388 cm − 1 assigned to out-of-plane C–H bending and ring-skeletal deformation consistent with the trisubstituted benzene ring of the linker.

In the Zn-BDC-NH2 MOF spectrum, the carboxylic C = O band of the free linker was replaced by a strong band at 1657.7 cm − 1 with a second band at 1587 cm − 1, assigned to the asymmetric carboxylate stretch, vas(COO−), together with a corresponding symmetric carboxylate stretch, vs(COO−), at 1383.1 cm − 1. Applying the empirical correlation of Deacon and Phillips (1980) between the asymmetric–symmetric carboxylate separation (Δv) and coordination geometry, the observed separation (Δv ≈ 275 cm − 1) is consistent with a bridging coordination mode of the carboxylate oxygens to Zn2+. Bands at 1319.3 and 1257.0 cm − 1, retained from the free –NH2 group, confirmed that the amine functionality survived synthesis, while new low-frequency bands at 685.0, 570.2, and 508.8 cm − 1, absent from the free-linker spectrum, were assigned to Zn–O stretching, providing direct evidence of metal–carboxylate coordination and successful framework formation, consistent with the Zn–O bonding reported for related Zn(BDC)-type frameworks (Li et al., 1998).

An analogous pattern was observed for Cu-BDC-NH2 MOF: the carboxylic C = O band was replaced by a pair of intense bands at 1651.4 and 1583.1 cm − 1 (asymmetric COO− stretch) with corresponding symmetric stretches at 1420.6 and 1376.3 cm − 1, confirming deprotonation and coordination of the carboxylate groups to Cu2+ (Deacon & Phillips, 1980), at a separation comparable to that reported for other Cu–carboxylate environments, including Cu–glyphosate complexes (Undabeytia et al., 2002).

Retained –NH2 bands at 1296.6 and 1248.5 cm − 1 confirmed preservation of the amine group, while two low-frequency bands at 513.5 and 407.6 cm − 1, not present in the free linker, were assigned to Cu–O stretching, confirming successful Cu-BDC-NH2 MOF formation.

Table 1 summarizes the diagnostic FTIR band assignments for the free linker and the two synthesized MOFs. The consistent pattern observed for both metals — (i) disappearance of the free carboxylic C = O stretch and its replacement by a paired asymmetric/symmetric COO− doublet, confirming coordination of the –COOH groups to the metal centres per the diagnostic criteria of Deacon and Phillips (1980); (ii) retention of the C–N stretching bands of the –NH2 group in the 1240–1320 cm − 1 region in both MOFs; and (iii) emergence of new sub-600 cm − 1 bands assigned to M–O stretching — is consistent with the successful synthesis of amine-functionalized Zn- and Cu-based MOFs through the reticular self-assembly of metal ions and carboxylate linkers described by Yaghi et al. (2003).

Table 1
Summary of principal FTIR band assignments (cm^{-1})

Assignment	BDC-NH2 linker	Zn-BDC-NH2 MOF	Cu-BDC-NH2 MOF
v(O–H/N–H), broad	3433	3548 (env.)	3550 (env.)
vas(COO−)/aromatic C = C	1633	1657.7 / 1587	1651.4 / 1583.1
vs(COO−)	–	1383.1	1420.6 / 1376.3
v(C–N), –NH2 retained	–	1319.3 / 1257.0	1296.6 / 1248.5
C–H/ring bending	1027.5	1204.6–1027.0	1176.7–1015.2
M–O stretching	–	685.0 / 570.2 / 508.8 (Zn–O)	513.5 / 407.6 (Cu–O)

3.3 X-ray Diffraction (XRD) Analysis

Powder XRD patterns of Zn-BDC-NH2 MOF and Cu-BDC-NH2 MOF were recorded over 2θ = 2–70°. Zn-BDC-NH2 MOF displayed sharp, well-resolved low-angle reflections, with the most intense peak at 2θ = 8.74° (d = 10.11 Å), indexed to the (101) plane, accompanied by a weaker reflection at 2θ = 7.84° (d = 11.27 Å), indexed to (002). This low-angle-dominated pattern is characteristic of layered Zn(BDC)-type frameworks, in which the (00l) and (101) reflections arise from periodic stacking of metal–carboxylate sheets (Li et al., 1998). Two further moderate-intensity reflections were observed at 2θ = 26.44° (100) and 29.32° (200), while higher-order (220), (300), and (311) reflections were only weakly developed beyond 2θ = 30°.

Cu-BDC-NH2 MOF displayed seven distinct sharp reflections — at 2θ = 9.30° (002), 24.46° (100), 27.06° (101, most intense), 28.54° (200), 36.14° (220), 45.44° (300), and 65.16° (311) — extending to considerably higher diffraction angles than Zn-BDC-NH2 MOF, indicating a comparatively higher degree of long-range crystallographic order.

Average crystallite sizes, estimated from the Debye–Scherrer equation, $D = K\lambda/(\beta\cos\theta)$ ($K = 0.9$, $\lambda = 1.5406$ Å; Patterson, 1939), using the FWHM of the most intense reflection of each sample, were ≈ 80 nm for Zn-BDC-NH2 MOF and ≈ 51 nm for Cu-BDC-NH2 MOF; these should be regarded as order-of-magnitude approximations given the 0.02° step size of the recorded data.

Both diffractograms confirm that the products are crystalline, with sharp reflections clearly distinguishable from the amorphous background and from the patterns of the unreacted metal salts, supporting formation of ordered coordination frameworks in both cases — a criterion also used by Naghdi et al. (2023) to confirm crystallinity in glyphosate-adsorbing MOFs. The greater number of well-resolved, higher-angle reflections for Cu-BDC-NH2 MOF relative to the intense but comparatively narrower low-angle-dominated pattern of Zn-BDC-NH2 MOF reflects differing nucleation and growth kinetics of Zn2 + and Cu2 + with the carboxylate linker under identical synthesis conditions, and mirrors the morphological differences observed by SEM (Section 3.4).

3.4 Scanning Electron Microscopy (SEM) Analysis

SEM micrographs of Zn-BDC-NH2 MOF revealed irregular, angular, plate-like/blocky particles extensively agglomerated into micron-scale clusters with rough, fractured-looking surfaces; individual sub-units were difficult to resolve as discrete, well-faceted crystals owing to the extent of aggregation.

In marked contrast, Cu-BDC-NH2 MOF micrographs showed a fine, densely packed morphology of near-spherical/globular nanoparticle sub-units arranged in coral-like or cauliflower-like clusters, considerably smaller and more uniform than the coarse Zn-BDC-NH2 MOF aggregates, with a correspondingly higher degree of fine-scale surface roughness and inter-particle porosity.

This clear morphological contrast — coarse, blocky, plate-like Zn-BDC-NH2 MOF versus fine, globular, densely clustered Cu-BDC-NH2 MOF — mirrors the crystallinity trend established by XRD and is consistent with the differing nucleation and growth behaviour of Zn2 + and Cu2 + under identical solvothermal conditions. The finer, more granular Cu-BDC-NH2 MOF morphology suggests a potentially larger accessible external surface area than the coarser Zn-BDC-NH2 MOF, a relationship between particle morphology and surface accessibility also noted for hierarchically structured glyphosate-adsorbing MOFs by Naghdi et al. (2023); this remains, however, a qualitative SEM-based inference that should be confirmed quantitatively by BET surface-area analysis in future work.

3.5 Comparative Structural Summary

The principal structural and morphological findings from the FTIR, XRD, and SEM analyses of the two MOFs are summarized in Table 2. Overall, the FTIR results confirm that both frameworks were synthesized successfully with the amine functional group intact, while the XRD and SEM results indicate that, under the conditions employed, Cu-BDC-NH2 MOF developed a somewhat higher degree of crystallinity and a finer particle morphology than Zn-BDC-NH2 MOF. These structural differences provide a basis for interpreting and anticipating differences in the pollutant-adsorption behaviour of the two amine-functionalized frameworks.

Table 2
Comparative structural summary of Zn-BDC-NH2 MOF and Cu-BDC-NH2 MOF

Property	Zn-BDC-NH2 MOF	Cu-BDC-NH2 MOF
Carboxylate bands (vas/vs COO−)	1657.7 / 1383.1 cm^{-1}	1651.4 / 1420.6 cm^{-1}
Metal–oxygen band(s)	570.2, 508.8 cm^{-1} (Zn–O)	513.5, 407.6 cm^{-1} (Cu–O)
–NH2 group retained	Yes (1319.3, 1257.0 cm^{-1})	Yes (1296.6, 1248.5 cm^{-1})
Most intense XRD reflection	(101) at 2θ = 8.74°	(101) at 2θ = 27.06°
No. of resolved XRD reflections	4	7
Crystallite size (Scherrer)	≈ 80 nm	≈ 51 nm
SEM morphology	Blocky, angular, plate-like aggregates	Fine, globular nanoparticle clusters

4. Conclusion

Amine-functionalized Zn-BDC-NH2 and Cu-BDC-NH2 metal–organic frameworks were reproducibly synthesized from a common linker, 2-aminoterephthalic acid, and their respective metal-nitrate precursors, using a simple, low-cost, buffered solution-based route conducted at room temperature. FTIR spectroscopy confirmed that both syntheses proceeded through deprotonation and coordination of the linker carboxylate groups to the metal centres, evidenced by new asymmetric/symmetric COO− doublets and metal–oxygen stretching bands, while the retained C–N bands of the –NH2 group in both products confirmed that the intended amine functionality survived framework assembly. Powder XRD confirmed the crystallinity of both products and revealed that Cu-BDC-NH2 MOF possessed a greater degree of long-range crystalline order and a smaller crystallite size than Zn-BDC-NH2 MOF, consistent with the markedly different SEM morphologies observed for the two materials — coarse, blocky aggregates for the zinc-based framework versus fine, globular nanoparticle clusters for the copper-based framework. These findings establish a validated, reproducible synthetic route to two structurally distinct, amine-bearing MOFs that are suitable candidates for pollutant-adsorption applications, the evaluation of which is reported in a companion study.

Declarations

Ethics, Consent to Participate, and Consent to Publish declarations

not applicable.

Funding:

The authors declare that no funding was received for this study.

Author Contribution

Charles Dike and Tunde conceived and designed the study, synthesized the MOFs, and wrote the main manuscript text. Olufunsho Abosede supervised the work / contributed to data analysis and interpretation of the FTIR, XRD and SEM results.

Data availability:

All data generated or analysed during this study are included in this published article.

References

1. Batten SR, Champness NR, Chen X-M, Garcia-Martinez J, Kitagawa S, Öhrström L, O'Keeffe M, Suh MP, Reedijk J. Terminology of metal–organic frameworks and coordination polymers (IUPAC Recommendations 2013). Pure Appl Chem. 2013;85(8):1715–24. https://doi.org/10.1351/PAC-REC-12-11-20.
2. Cohen SM. Postsynthetic methods for the functionalization of metal–organic frameworks. Chem Rev. 2012;112(2):970–1000. https://doi.org/10.1021/cr200179u.
3. Deacon GB, Phillips RJ. Relationships between the carbon–oxygen stretching frequencies of carboxylato complexes and the type of carboxylate coordination. Coord Chem Rev. 1980;33(3):227–50. https://doi.org/10.1016/S0010-8545(00)80455-5.
4. Deng H, Doonan CJ, Furukawa H, Ferreira RB, Towne J, Knobler CB, Wang B, Yaghi OM. Multiple functional groups of varying ratios in metal–organic frameworks. Science. 2010;327(5967):846–50. https://doi.org/10.1126/science.1181761.
5. Furukawa H, Cordova KE, O'Keeffe M, Yaghi OM. The chemistry and applications of metal–organic frameworks. Science. 2013;341(6149):1230444. https://doi.org/10.1126/science.1230444.
6. Li G-P, Zhang K, Zhang P-F, Liu W-N, Tong W-Q, Hou L, Wang Y-Y. Thiol-functionalized pores via post-synthesis modification in a metal-organic framework with selective removal of Hg(II) in water. Inorg Chem. 2019;58(5):3409–15. https://doi.org/10.1021/acs.inorgchem.8b03505.
7. Li H, Eddaoudi M, Groy TL, Yaghi OM. Establishing microporosity in open metal–organic frameworks: Gas sorption isotherms for Zn(BDC) (BDC = 1,4-benzenedicarboxylate). J Am Chem Soc. 1998;120(33):8571–2. https://doi.org/10.1021/ja981669x.
8. Li J-R, Sculley J, Zhou H-C. Metal–organic frameworks for separations. Chem Rev. 2012;112(2):869–932. https://doi.org/10.1021/cr200190s.

9. Naghdi S, Brown E, Zendehbad M, Duong A, Ipsmiller W, Biswas S, Toroker MC, Kazemian H, Eder D. Glyphosate adsorption from water using hierarchically porous metal–organic frameworks. Adv Funct Mater. 2023;33(20):2213862. https://doi.org/10.1002/adfm.202213862.
10. Patterson AL. The Scherrer formula for X-ray particle size determination. Phys Rev. 1939;56(10):978–82. https://doi.org/10.1103/PhysRev.56.978.
11. Rubio-Martinez M, Avci-Camur C, Thornton AW, Imaz I, Maspoch D, Hill MR. New synthetic routes towards MOF production at scale. Chem Soc Rev. 2017;46:3453–80. https://doi.org/10.1039/C7CS00109F.
12. Stock N, Biswas S. Synthesis of metal-organic frameworks (MOFs): Routes to various MOF topologies, morphologies, and composites. Chem Rev. 2012;112(2):933–69. https://doi.org/10.1021/cr200304e.
13. Undabeytia T, Morillo E, Maqueda C. FTIR study of glyphosate–copper complexes. J Agric Food Chem. 2002;50(7):1918–21. https://doi.org/10.1021/jf010988w.
14. Wu J, Zhou J, Zhang S, Alsaedi A, Hayat T, Li J, Song Y. Efficient removal of metal contaminants by EDTA modified MOF from aqueous solutions. J Colloid Interface Sci. 2019;555:403–12. https://doi.org/10.1016/j.jcis.2019.07.108.
15. Yaghi OM, O'Keeffe M, Ockwig NW, Chae HK, Eddaoudi M, Kim J. Reticular synthesis and the design of new materials. Nature. 2003;423(6941):705–14. https://doi.org/10.1038/nature01650.
16. Zhang N, Yuan L-Y, Guo W-L, Luo S-Z, Chai Z-F, Shi W-Q. Extending the use of highly porous and functionalized MOFs to Th(IV) capture. ACS Appl Mater Interfaces. 2017;9(30):25216–24. https://doi.org/10.1021/acsami.7b04192.
17. Zhao M, Huang Z, Wang S, Zhang L, Zhou Y. Design of L-cysteine functionalized UiO-66 MOFs for selective adsorption of Hg(II) in aqueous medium. ACS Appl Mater Interfaces. 2019;11(50):46973–83. https://doi.org/10.1021/acsami.9b17508.

Figures

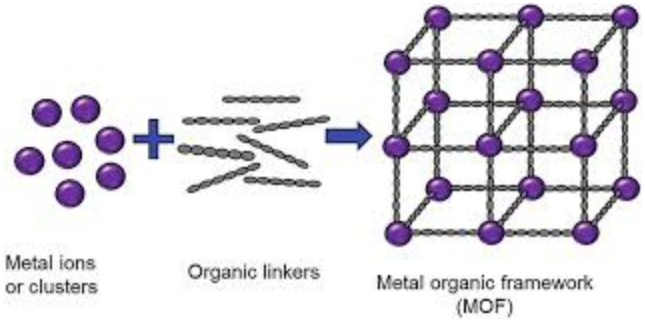


Figure 1

Structure of the metal ions and organic linker (2-aminoterephthalic acid, BDC-NH2) used for MOF synthesis.

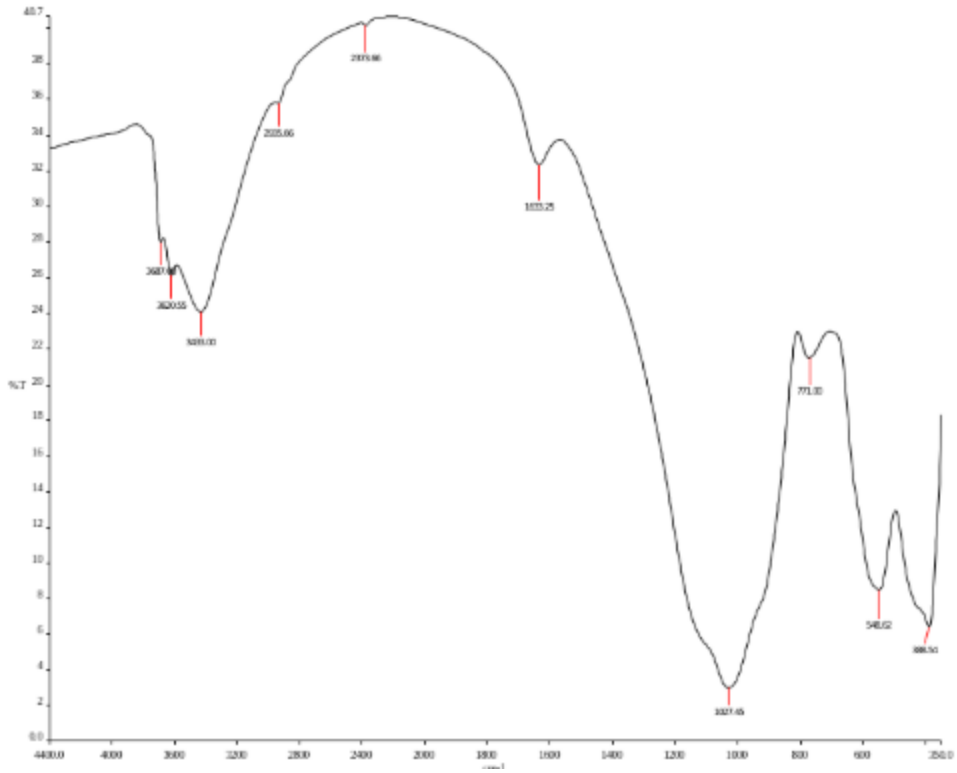


Figure 2

FTIR spectrum of the BDC-NH2 organic linker.

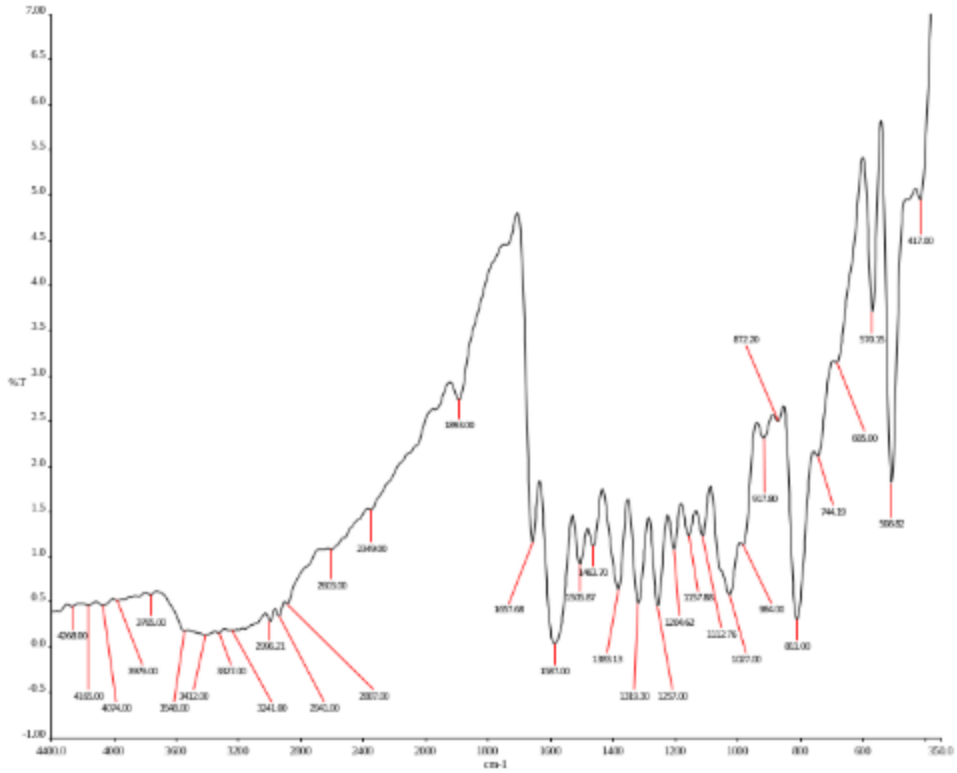


Figure 3

FTIR spectrum of the synthesized Zn-BDC-NH2 MOF.

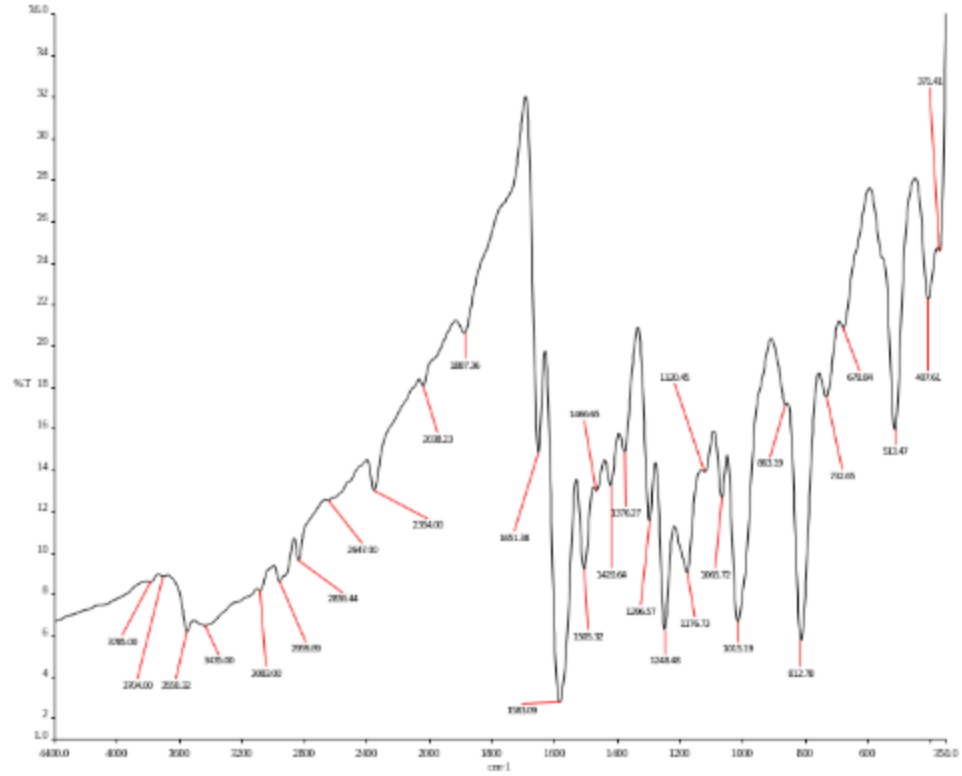


Figure 4

FTIR spectrum of the synthesized Cu-BDC-NH2 MOF.

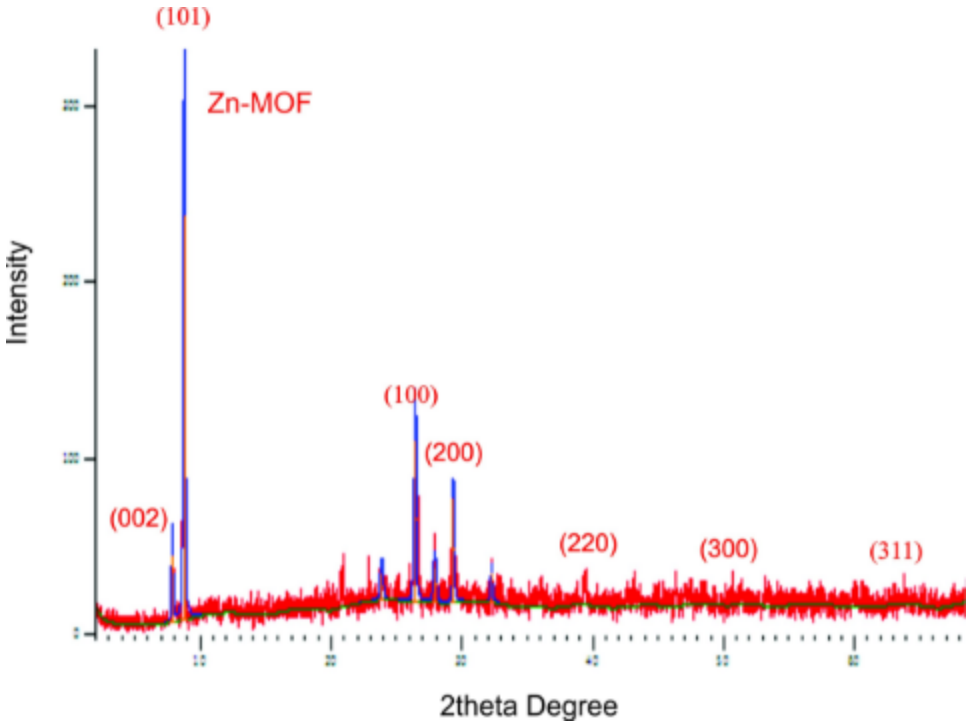


Figure 5

XRD diffractogram of the synthesized Zn-BDC-NH2 MOF.

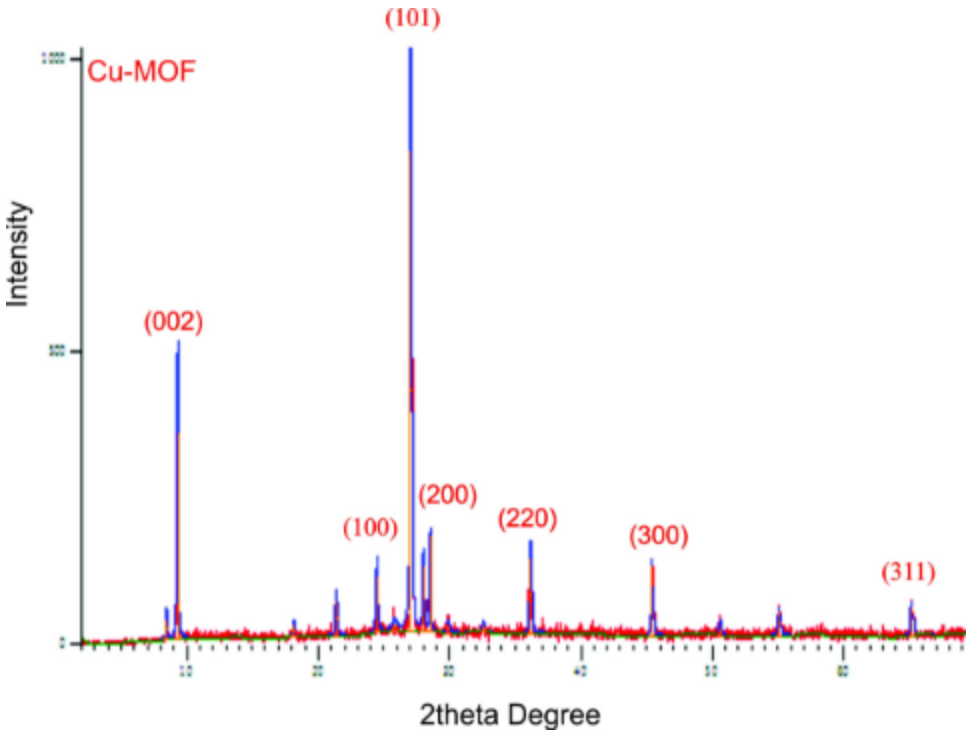


Figure 6

XRD diffractogram of the synthesized Cu-BDC-NH2 MOF.

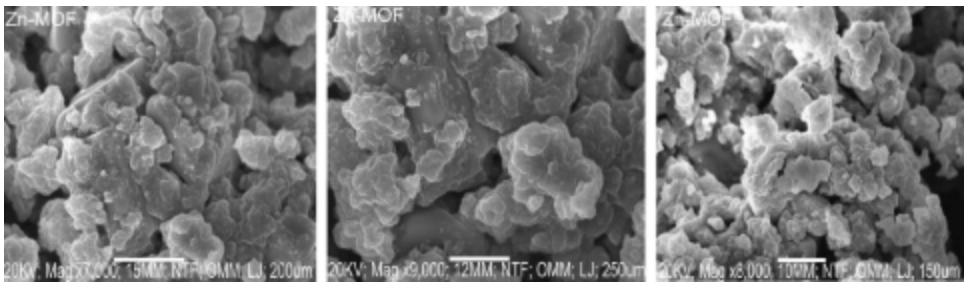


Figure 7

SEM micrographs of Zn-BDC-NH2 MOF at ×7,000–×9,000 magnification.

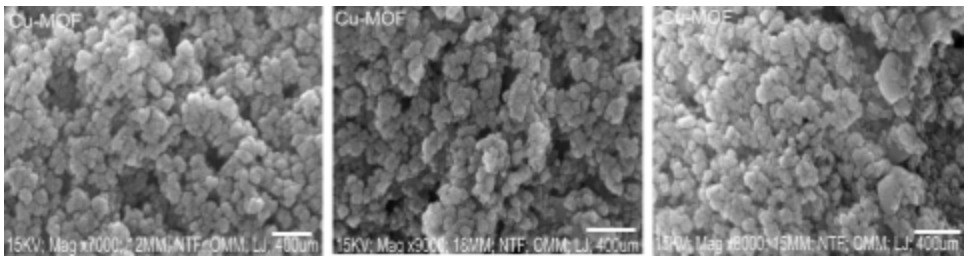


Figure 8

SEM micrographs of Cu-BDC-NH2 MOF at ×7,000–×9,000 magnification.